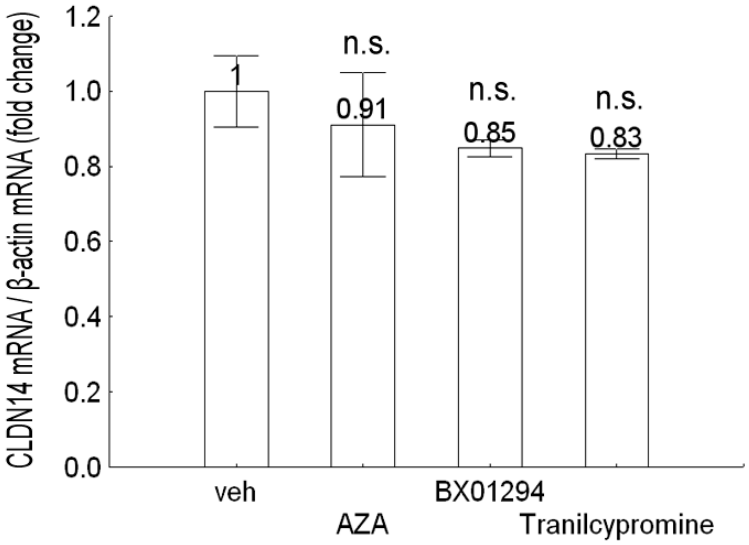

Figure S1. Epigenetic effects on claudin-14 mRNA levels in primary cultures of mouse TALH cells. The mouse TALH cells were cultured for 16hrs in presence of 5μM 5-Aza-2′-deoxycytidine (AZA), 0.1μM BIX 01294 and 10μM tranylcypromine respectively, assayed for CLDN14 mRNA levels with real-time PCR, normalized to β-actin mRNA, and compared to vehicle treatments (N=3).

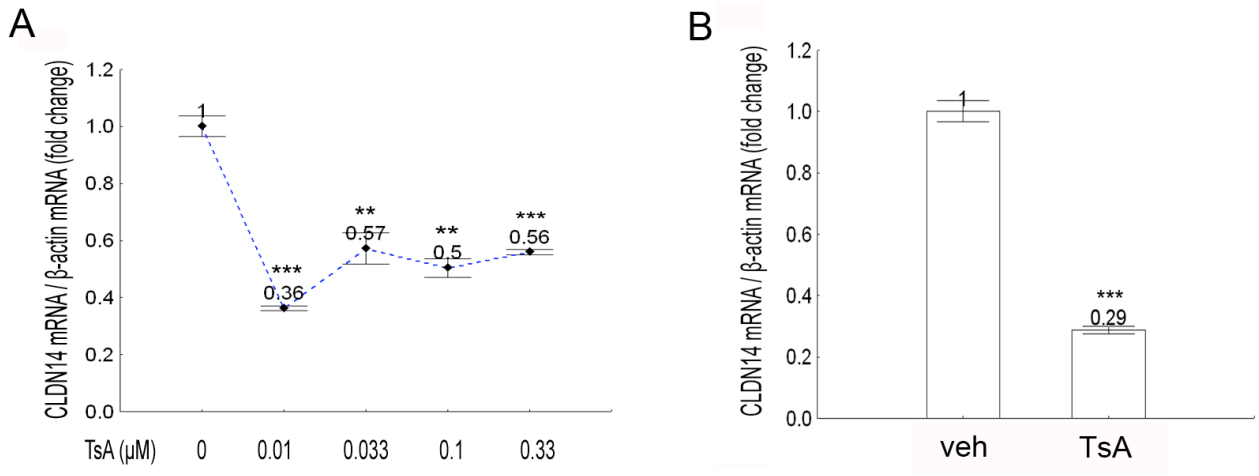

Figure S2. TsA effects on claudin-14 gene expression in vitro and in vivo in the kidney. (A) The TsA effects on CLDN14 mRNA levels in primary cultures of mouse TALH. (B) The TsA effects on CLDN14 mRNA levels in mouse kidneys.

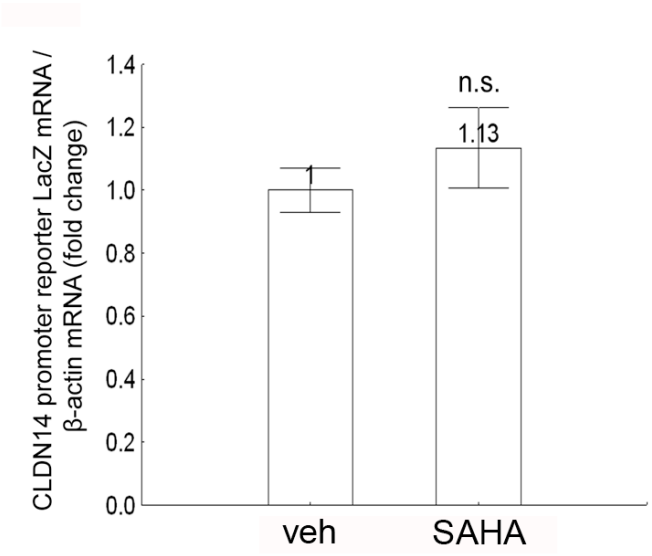

Figure S3. The effects of SAHA on claudin-14 promoter activity. The mRNA levels of lacZ gene were measured from the CLDN14$^{lacZ/+}$ reporter mouse kidneys receiving SAHA or vehicle treatments.

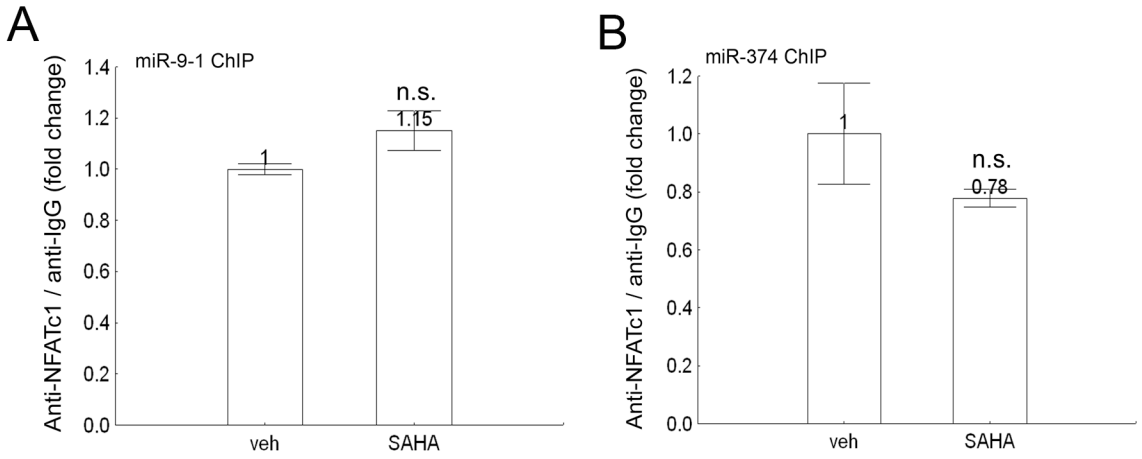

Figure S4. SAHA effects on NFATc1 binding to microRNA promoters. Wild-type C57BL/6 mice were treated with 25mg/kg BW^{-1} SAHA for 4hrs and assayed for NFATc1 binding affinity to miR-9-1 (A) and miR-374 (B) gene promoters in the kidney with ChIP (N=5).

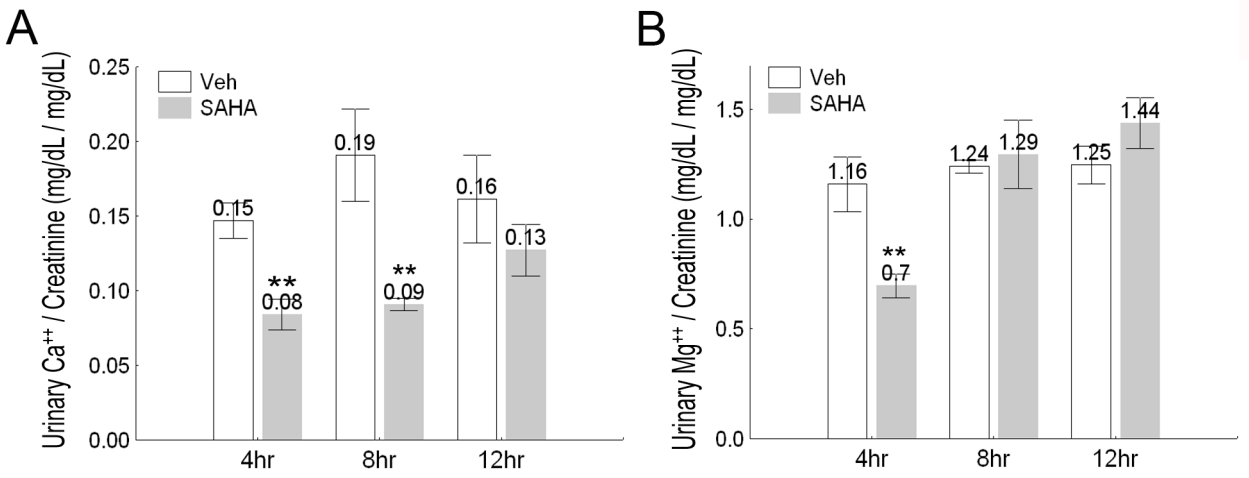

Figure S5. The time response of SAHA effects on urinary excretion of Ca^{++} and Mg^{++}. The urinary excretion rates for Ca^{++} (A) and Mg^{++} (B) in WT mice treated with SAHA or vehicle from spot urine collections were shown as ratios to urinary creatinine levels.

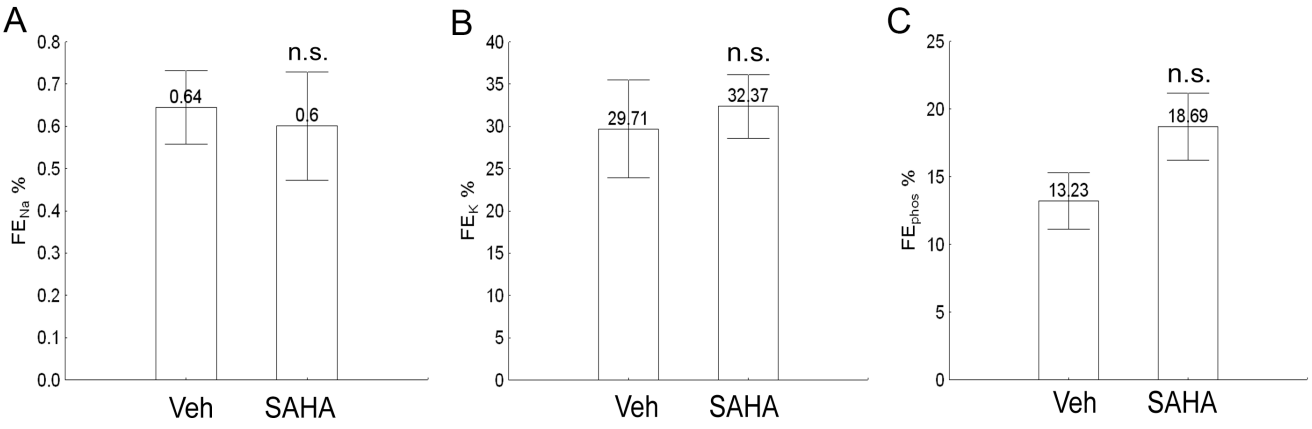

Figure S6. The effects of SAHA on fractional excretion rates for Na^+, K^+ and phosphate. Wild-type C57BL/6 mice were treated with 10mg/kg BW^{-1} SAHA per day and analyzed for changes in 24hr urinary fractional excretion rates of Na^+ (FE_{Na}; A), K^+ (FE_K; B) and phosphate (FE_{phos}; C) (N=9).

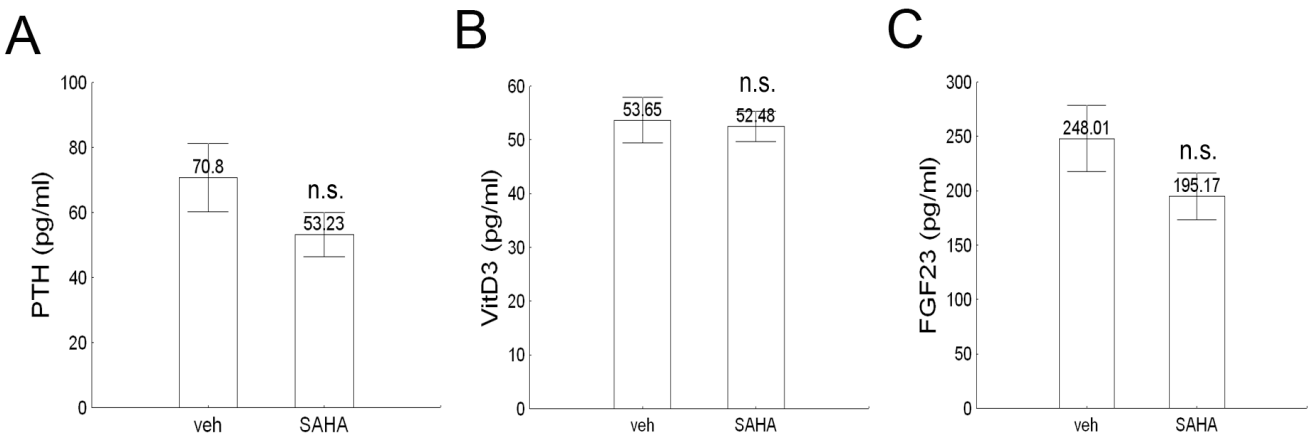

Figure S7. Circulating hormonal levels in SAHA versus vehicle treated mouse kidneys. Serum PTH (A), 1,25-$(OH)_2$-vitD_3 (B) and FGF23 (C) levels were measured with ELISA and shown as mean ± SEM, n=5.

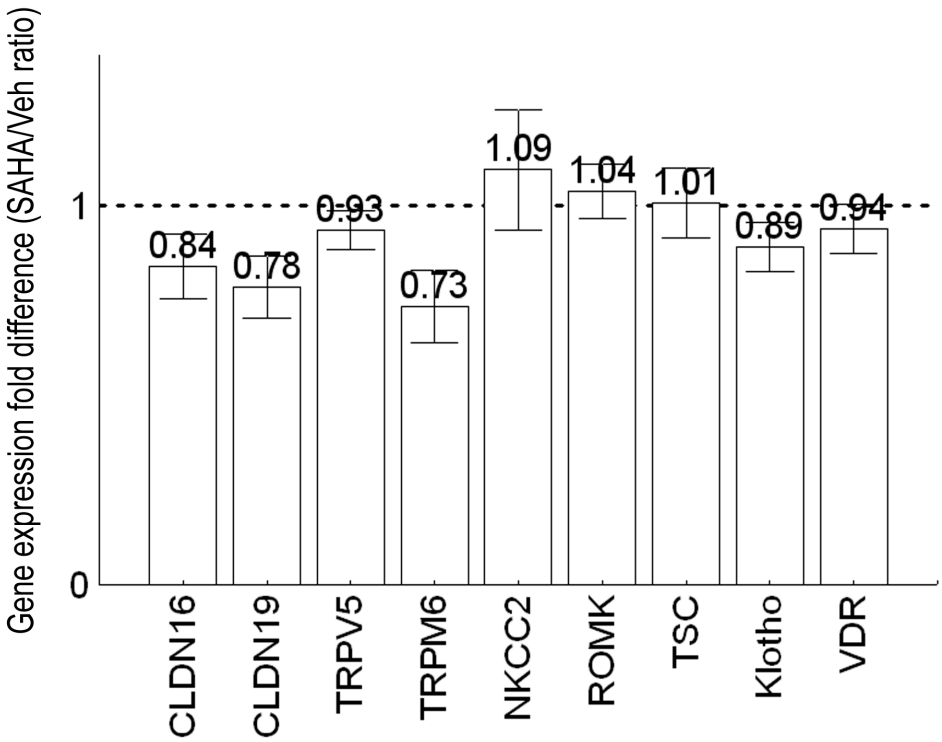

Figure S8. Gene expression analyses of renal ion transporters in SAHA versus vehicle treated mouse kidneys by real-time PCR. Values are shown as fold ratios relative to the vehicle level (as mean ± SEM; n=5).

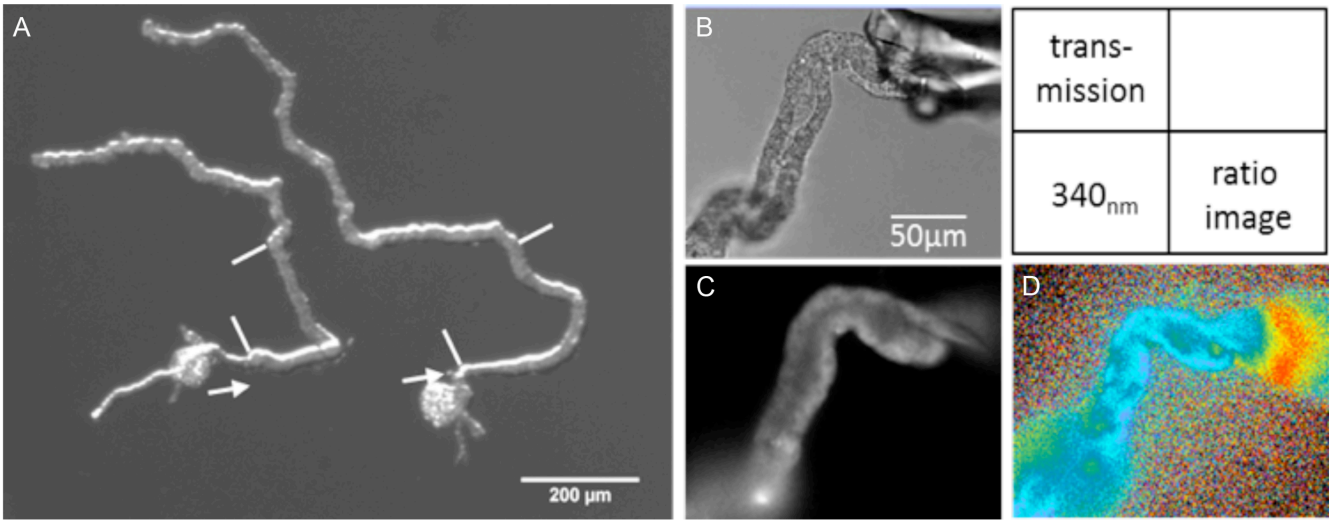

Figure S9. Intracellular Ca^{++} recording in perfused DCT tubules. (A) Representative micro-dissected DCT tubules. Arrow indicates perfusion direction; white lines denote the starting and the ending positions of each perfused segment. (B) Bright-field image of a perfused DCT tubule. (C) Fluorescence image captured at 340nm. (D) Ratio image captured at 340 nm versus 380 nm.